THE PENNSYLVANIA STATE UNIVERSITY

SCHREYER HONORS COLLEGE

DEPARTMENT OF CHEMICAL ENGINEERING

# Sterile Filtration of Vaccines: The Effect of Formulations and Differences in Hydrophobicity

ALEX WEE

Spring 2023

A thesis

submitted in partial fulfillment

of the requirements

for a baccalaureate degree

in Chemical Engineering

with honors in Chemical Engineering

Reviewed and approved* by the following:

Andrew Zydney

Professor of Chemical Engineering

Thesis Supervisor

Michael Janik

Department Head of Chemical Engineering

Honors Adviser

* Electronic approvals are on file.

# Abstract

The recent COVID-19 pandemic demonstrated the importance of vaccine development. Novel vaccine developments and strategies are becoming increasingly important in the pathogenic arms race as the world population continues to rise. One of the critical steps in the production of these vaccines is the final sterile filtration, which is needed to insure the sterility of the injectable product. Despite growing progress in the vaccine field, much of the mechanics and factors behind the sterile filtration process of vaccines are still poorly understood. Recent studies have demonstrated the importance of several factors in the vaccine filtration process, including the surfactant concentration and membrane pore size, both of which affect the filtration efficacy in terms of fouling and vaccine yield.

The objectives of this thesis were to: (1) quantify the hydrophobicity for several common sterile filter membranes used in industry, (2) to determine whether relative hydrophobicity differences between surfactants and membranes affects the filtration efficacy of a vaccine products. Experiments investigated the behavior of several sterile filters, including the Sartobran P, Supor EKV, Sterilux, and Stylux, with the surfactants Tween 20, Poloxamer 188, and Cetyltrimethyl ammonium bromide (CTAB). Data were obtained with a nanoparticle suspensions that has previously been shown to have high similarities to the filtration behavior of a live-attenuated virus vaccine formulation.

The experimental studies demonstrated that the presence of a surfactant is necessary to reduce membrane fouling and achieve adequate particle transmission. Poloxamer 188 caused higher rates of fouling than either Tween 20 or CTAB. of the best performance was obtained with the Sartobran P membrane using Tween 20, which showed a filter capacity of more than 450 $L/m^2$ in throughput. Hydrophobicity differences between the membrane and surfactant showed

minimal correlation with either the fouling rate or particle transmission. The Stylux membrane showed very high rates of particle transmission when used in the presence of Tween 20.. These results provide important insights into some of the factors controlling the sterile filtration of viral vaccine products.

# Table of Contents

**Acknowledgements** ..... **iv**

**1. Introduction** ..... **1**

**2. Materials and Methods** ..... **5**

2.1. Buffer and Surfactants ..... 5

2.2. Sterile Filters ..... 6

2.3. Hydrophobicity Determination of the Sterile Filters ..... 6

2.4. Model Polystyrene Nanoparticles ..... 7

2.5. Sterile Filtration ..... 7

2.6. Nanoparticle Fluorescence Measurements ..... 8

2.7. Development of a Calibration Curve ..... 9

**3. Results and Discussion** ..... **10**

3.1. Hydrophobicity Determination ..... 10

3.2. Comparison of 80:20 Mix to Literature Data ..... 15

3.3. Fouling Behavior for Different Filter and Surfactant Combinations ..... 17

3.4. Nanoparticle Transmission ..... 21

**4. Conclusion** ..... **26**

**5. References** ..... **29**

# Acknowledgements

I would like to thank my mentors, friends, and family for supporting me through the duration of this project. The multitude of people that assisted me physically, mentally, and emotionally through my endeavors made this possible.

I would like to give special thanks to Dr. Andrew Zydney. His support over the years has been invaluable. He has instilled within me an appreciation for the scientific process and chemical engineering that I believe is integral to my success as a student and as a person. Lastly, I'd like to thank him for taking a chance on the inexperienced freshman that emailed him.

I would also like to give special thanks to Dr. Neil Taylor. Neil taught me much of what I know about working in a laboratory. His infinite patience in guiding me through my biggest mistakes and his advice for both life and the lab were both admirable and vital to my growth.

To all of the graduate students in the Zydney Lab, with special thanks to Mohammad Afzal, Kevork Oliver Messerian, and Zhuoshi Du, I extend my sincerest gratitude. I cannot imagine a more loving and welcoming group of people to populate a laboratory.

Finally, I would like to thank my mother. She supported me and believed in me at times when I did not even believe in myself. I would not be half the man I am today without her in my life.

# 1. Introduction

Vaccines are an integral part of modern healthcare. Vaccine prevalence in global healthcare programs is immense, with the World Health Organization predicting an estimated 2-3 million lives saved each year due to immunization [1]. Given the prevalence of vaccines, it is important to understand how they work within people. The human body has innate and adaptive immune responses. Innate responses are general protective measures that function continually as an initial line of defense against pathogens. This class of responses works in tandem with the adaptive system. The adaptive responses involve the recognition of antigens by T and B cells, which promptly create antibodies to fight the pathogen. This is the process that vaccines seek to utilize in administering preventative healthcare [2]. Vaccines are composed of antigens that are derived from the pathogen they protect against, or synthetic analogs to that antigen, which will stimulate the same immune responses when introduced to the body, but at a lower scale than a full pathogenic attack.

Vaccines also have a major economic impact in addition to their healthcare benefits. Poverty can be perpetuated due to infectious disease. For example, in sub-Saharan Africa, families that are affected by a single case of meningococcal meningitis can launch the entire family into a spiral of poverty as the family's income is spent on healthcare [3]. As such, there are hidden economic benefits to preventative healthcare. A cost-benefit analysis for expedited vaccine rollout found that vaccination of 40% of the world by 2021 would cost roughly $50 billion USD, but would create a value of about $9 trillion globally [4]. Additionally, vaccines are a major market on their own. In 2020 the global vaccines market was at $55.44 billion USD and is projected to grow to $125.49 billion USD by 2028 [5]. The recent COVID epidemic has boosted vaccine economic growth as well. Pfizer, one of the major COVID-19 vaccine

purveyors, reports a revenue of $81.288 billion USD in 2021, which is roughly double the revenue it had in 2020 [6]. Moderna also reported similar revenue increases, going from $803 million USD in 2020 to $1.8 billion USD in 2021 [7]. The market for COVID vaccines may decline somewhat as the world gains immunity but these vaccines will remain vital to world health as the virus continues to mutate, necessitating boosters or further vaccinations.

Vaccine manufacture and processing is a complicated series of steps. There is risk imposed by the near-infinite variability in the starting materials, microorganisms, production environments, and other factors surrounding development [8]. The first step in the production of traditional viral vaccines is the culturing or expression of an antigen or virus within a host. This typically involves the use of animal cells. Live-attenuated viral vaccines, such as the yellow fever vaccine YF-17D, typically pass virus cells through a series of in vitro cell cultures involving monkey cells or chicken embryonic tissues [9]. Recent developments have opened the possibility of plant-based vaccines as well, with influenza and COVID-19 plant-based vaccines showing promising results for commercialization [10].

After initial antigen or virus propagation, the vaccine products must be processed to remove impurities. It is imperative that vaccines include sterility assurance, as the presence of foreign bacteria could have potentially catastrophic effects on the human body. Some forms of sterilization, such as heat or ethylene oxide sterilization, pose inherent risk to the viability of the vaccine product, as they may destroy the antigens or live-attenuated viruses. As such, the most common method for sterilization of viral vaccines is sterile filtration. Sterile filters used for aseptic processing are rated at 0.2 μm pore size or smaller, and have been shown to retain even the smallest bacteria (which can be somewhat less than 1 μmin diameter [11]). These filters are typically classified as “sterilizing grade” based on their ability to retain at least 107 CFU per $cm^2$

of filter area of Brevundimonas diminuta [12], which is one of the smallest known bacteria with approximately 0.3 μm diameter [13].

The 0.2 μm pore size in standard sterile filters poses some challenges for many vaccines since the size of the vaccine particles or viruses are similar to, or in some cases even larger than, the pore size of these membranes. When these large particles encounter the smaller pores, the filter experiences extreme fouling, which leads to reduced filter capacity for undesirable biomaterial and significant yield loss for the vaccine product. This makes sterile filtration impossible in certain cases, such as the preparation of 2-4 micron particles included in some novel tumor vaccines [14].

Reports of successful sterile filtration of large particle vaccines do exist despite the physical limitations presented by the 0.2 μm pore size. For example, Taylor et. al demonstrated that it was possible to sterile filter a live inactivated cytomegalovirus vaccine candidate with particle size ranging from 100-450 nm, but only with some sterile filters [15]. In this study, transmission of the vaccine product ranged anywhere from 1% to 80% depending on the sterile filter used. In another study conducted by Pazouki et. al, polystyrene nanoparticles ranging from 40-600 nm were successfully filtered through sterile filtration membranes [16]. Both of these studies demonstrated better sterile filtration performance in the presence of nonionic surfactants that are known to reduce hydrophobic interactions, suggesting that size exclusion effects are not the only thing to consider when designing the sterile filtration process for specific vaccine candidates.

As a result of this, it is important to understand what factors actually determine the yield of a vaccine formulation during sterile filtration. Taylor et al. found that sterile filtration of live-attenuated virus vaccines was most successful when using multilayer filters (as compared to

filters having a single layer). Another study found that particle transmission decreased with increasing solution conductivity due to the increase in particle adsorption. Solution pH was also found to have a small effect on particle transmission, with transmission increasing with increasing pH [17]. The transmission of 200-400 nm particles through 0.2 μm pore size filters has been found to have no direct correlation with membrane morphology (homogeneous versus asymmetric) or membrane material (e.g., polyethersulfone versus cellulose acetate). Rather, the dominating effect appeared to be the pore size of the filters, as determined by bubble point data or mercury intrusion porosimetry [23].

The objectives of this thesis were to (1) characterize the hydrophobicity of various sterile filtration membranes typically utilized in industry, and (2) determine the effect of hydrophobicity on the sterile filtration process using a series of surfactants and sterile filtration membranes. Industry standard filters are all labeled as hydrophilic, with no other hydrophobicity rating included. As a result, it can be difficult to compare different filters in applications where hydrophobicity of the surface may be important. Additionally, there is little information on the magnitude of the hydrophobic interactions between the particles and membrane and its effects on both particle yield and membrane fouling.

# 2. Materials and Methods

## 2.1. Buffer and Surfactants

Phosphate buffered saline (PBS) was purchased from Thermo Fisher as a 10x and 20x concentrate. In both cases, the PBS was typically prepared for experimental use in 1000 mL batches to create 1x PBS. In the 10x case, 100 mL of buffer was diluted with 900 mL of deionized (DI) water to achieve a final concentration of 10 mM phosphate, 137 mM NaCl, and 3 mM KCl. In the 20x case, 50 mL of buffer was diluted with 950 mL of DI water to achieve the same final concentrations. The diluted buffer was sterile filtered to remove any particulates before pH adjustment. The pH of the diluted buffer was adjusted to 7.8 using 1 M NaOH or 1 M HCl as needed, with the pH measured using a calibrated OakTon pH 700 pH meter.

Experiments were performed with various surfactants, several of which are commonly added to vaccine formulations as excipients to help stabilize the vaccine during storage and delivery to the patient. The nonionic surfactants, Tween 20 and Poloxamer 188, were purchased from Millipore Sigma. Cetyltrimethylammonium Bromide (CTAB) was the only positively-charged surfactant used. CTAB was purchased from MP Biomedicals as a powder. To prepare nanoparticle suspensions, each surfactant was added to 250 mL of PBS at concentrations above the critical micelle concentration for that particular surfactant: 250 µl of Tween 20 and Poloxamer 188 were used while 0.082 g of CTAB was used.

## 2.2. Sterile Filters

Various sterile filters were purchased and used in the experiments. Sterile filters that were bought as membrane disks were cut into 25 mm disks using a specially-designed cutting device. The cut membranes were then placed in a stainless-steel filter holder and sealed by an O-ring. All filters were used once. Sartobran P is a cellulose acetate filter obtained from Sartorius. Polyethersulfone filters used in the experiments included the Supor EKV KM2, Supor EAV, and Stylux. The Supor filters were sourced from Pall, while the Stylux was from Meissner. Two polyvinylidene fluoride filters (Sterilux and Durapore) were also investigated. Sterilux is produced by Meissner, while the Durapore is sourced from Millipore.

## 2.3. Hydrophobicity Determination of the Sterile Filters

The hydrophobicities of the sterile filters were evaluated using contact angle measurements, which provide a measure of water "spreading" on the membrane surface. Contact angles were measured in triplicate at the Materials Characterization Lab at the PSU Materials Research Institute using a Ramé-hart 260 Automated Goniometer / Tensiometer. Photos of water droplets as they came into contact with each filter were obtained. Contact angle data for the left and right sides of the droplets were averaged at each time point. These points were then plotted and fitted with a linear regression to obtain an "initial" contact angle value, which was used to estimate the relative hydrophobicity of the different filters. Higher contact angle values indicate a more hydrophobic filter, whereas lower values indicate a more hydrophilic filter.

## 2.4. Model Polystyrene Nanoparticles

Fluorescently labeled polystyrene latex particles were used as a model for a live-attenuated virus in this experiment following the work of Taylor et al. [15]. All particles were bought directly from Magsphere Inc. The particles were red and blue. The red particles were 200 nm, whereas the blue particles were 300 nm. The red particles had an excitation wavelength of 538 nm, and the blue particles had an excitation of 340 nm. The emission wavelengths were 584 and 400 nm, respectively. Nanoparticles were mixed in an 80:20 ratio, with the majority of the particles being the red (200 nm) particles at a total concentration of 1 x 1010 particles/mL. This mixture of particles was found to be an effective model for the sterile filtration of a viral vaccine product in terms of both the particle yield and fouling behavior [15].

## 2.5. Sterile Filtration

Sterile filtration experiments were done at a constant filtrate flux of 300 $L/m^2/hr$ (LMH) in triplicate. All sterile filters were placed downstream of a pressure gauge. The permeate end of the filters were open to the atmosphere, with permeate collected in 1 mL increments at specific time points to evaluate the particle transmission. The flux was maintained with a Masterflex L/S pump with Easy-Load II. Masterflex L/S 16 tubing used for the experiments. Figure 1 shows the general setup used for the experiments.

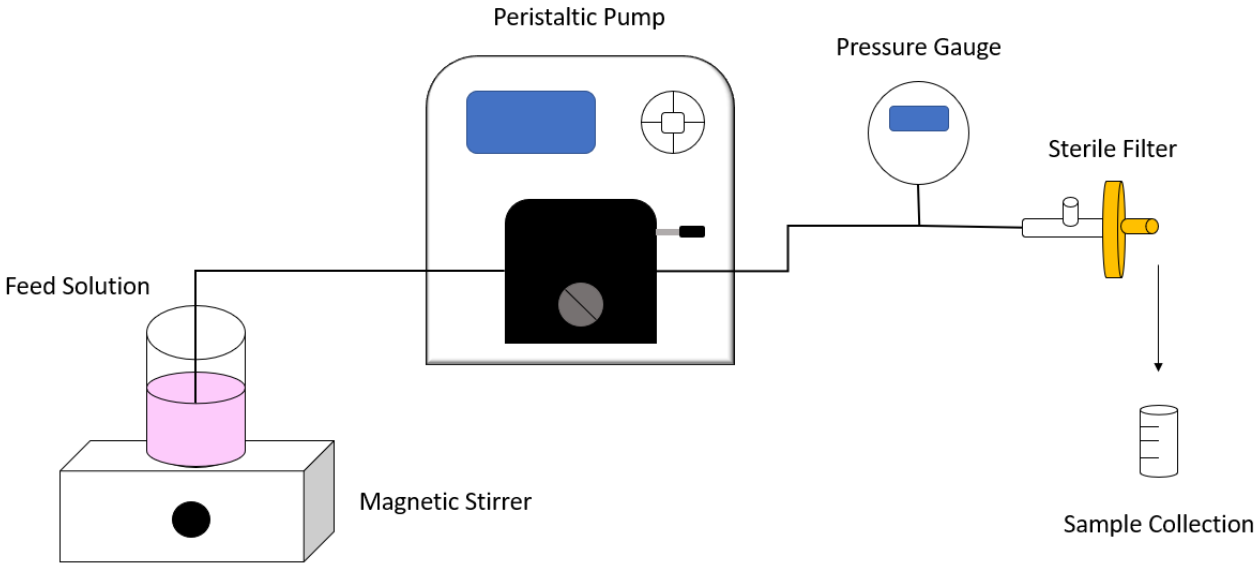


**Figure 1:** General experimental setup for filtration experiments. The stock nanoparticle solution was constantly stirred and fed through the pump at a constant rate. Inline pressure was measured by an Ashcroft pressure gauge. The filtrate exit from the sterile filter was open to the atmosphere, and samples were collected at set time intervals for subsequent analysis.

## 2.6. Nanoparticle Fluorescence Measurements

Permeate samples obtained from the experiments were analyzed for nanoparticle concentration based on the fluorescence intensity. Each sample, including the feed, was loaded into a Greiner black polystyrene microplate in duplicate. A Tecan Infinite M200 PRO was used to measure the fluorescence intensity, with the nanoparticle concentration determined using An appropriate calibration curve.

2.7. Development of a Calibration Curve

Nanoparticle concentrations were developed using a calibration curve constructed from a series of samples with known concentrations of nanoparticles. A mixture containing 1 x 1010 particles/mL was created with a 80:20 ratio of red to blue particles using 1x PBS. The dilutions used to create the calibration curve were as follows: 1x, 2x, 4x, 5x, 10x, 15x, 20x, where x denotes the ratio of nanoparticle solution to PBS. For example, 20x indicates that the nanoparticle solution was diluted to be 1/20th of the original concentration. After performing dilutions, each sample was plated in duplicate and measured for fluorescence intensity. Figure 2 depicts sample calibration curves created for both red and blue fluorescent nanoparticles.

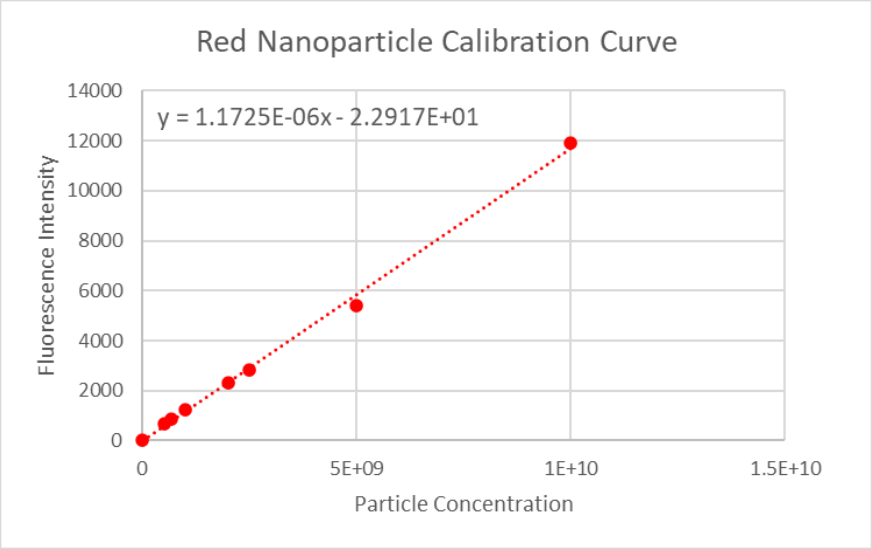

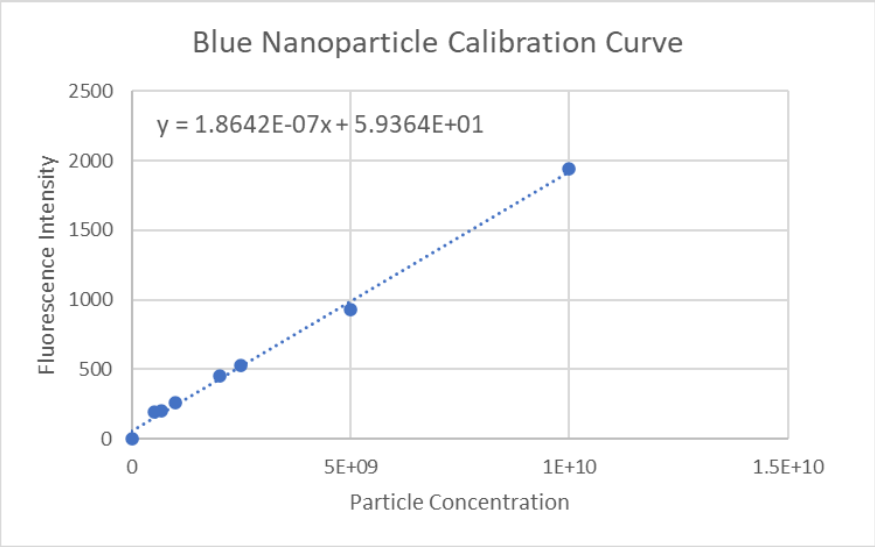


**Figure 2:** Calibration curves for the red and blue nanoparticles based on fluorescence intensities. Linear regression equations for the curves have been included on the graphs for ease of use.

The fluorescence intensity varied linearly with the nanoparticle concentration with R2 values greater than 0.99. The linear regression fits to the data were used to construct calibration curves, with the best fit linear equations used to estimate the concentration of particles based on the measured fluorescence intensity in both the feed and permeate samples.

# 3. Results and Discussion

## 3.1. Hydrophobicity Determination

The hydrophobicities of various industry sterile filtration membranes were determined through contact angle measurements. Sample images used for the contact angle analyses for the Durapore, Stylux, and Sterilux membranes are included in Figure 3.

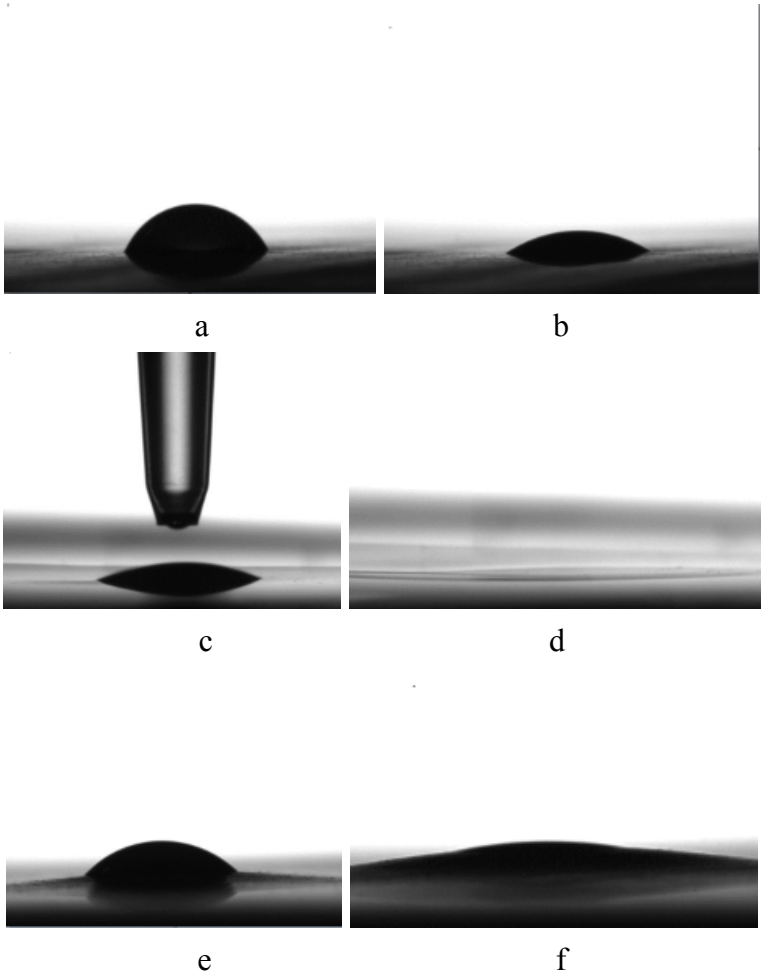


**Figure 3:** Close up images of various sterile filters during contact angle measurements. Images a, c, and e represent the Duapore, Stylux, and Sterilux immediately after water drop placement. Images b, d, and f represent the same filters several seconds after water drop placement.

The contact angle of each droplet, evaluated from both the left and right sides of the image, were logged and analyzed to determine the relative hydrophobicity of each filter. Initially, data obtained from the goniometer were plotted as a function of time, with the theoretical "initial" contact angle value determined by extrapolation of the data back to t = 0. The time dependence seen in the experimental data reflect the porosity of the sterile filters, with the water droplets rapidly intruding into the membrane pores causing the drop volume to decrease). This can be seen in Figure 3, where the water droplet disappears several seconds after placement. Typical results for the contact angle measurements of the Durapore membrane are shown in

Figure 4, with the contact angle of the Durapore filter evaluated as 64.6 degrees based on the intercept for the linear regression fit. Note that the reduction in contact angle with time reflects the decrease in the effective hydrophobicity of the membrane as more of the pores become filled with water.

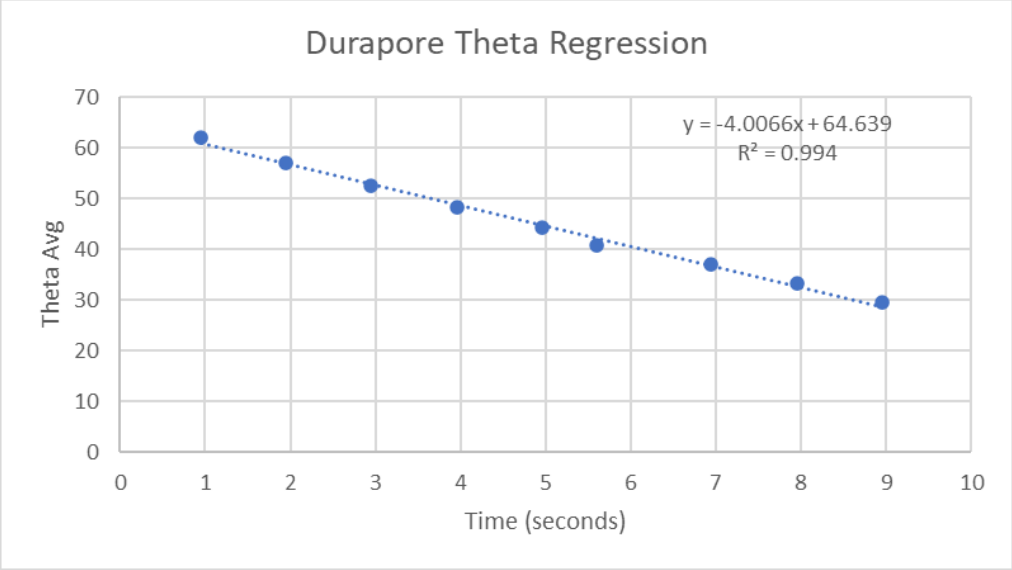


**Figure 4:** Contact angle data for the Durapore membrane. The estimated contact angle was obtained from the y-intercept of the linear regression fit, yielding a 64.6° contact angle for the Durapore.

While this approach worked well for certain sterile filters, other sterile filters provided extremely inconclusive data. The goniometer frequently returned error messages indicated that there was an "Error in Profile Data" (EIPD) or "Cannot Find Edge" (CFE). EIPD instances were caused by conditions in which the left or right contact angle of the droplet approached 180°. CFE instances seemed to occur when the machine's data collection started after the water droplet had already passed through the sterile filter, causing the machine to be unable to find the water droplet to measure. Due to this, the linear regression method could not be used to find contact angles for the Stylux, Sterilux, Supor EAV, or Sartobran P.

A different method for hydrophobicity determination was thus developed when the linear regression of the contact angle versus time data was ineffective. In this case, the first two or three data points were simply averaged, with this average value used as an approximation of the true contact angle. Table 1 summarizes the measured contact angles of the different membranes.

**Table 1:** Various Average Contact Angles for Sterile Filters

| **Sterile Filter** | **Average Contact Angle** |
|---|---|
| Supor EAV | N/A |
| Sterilux | 92 |
| Durapore | 83 |
| Stylux | 51 |
| Sartobran P | 45 |
| Supor EKV | 37 |

While each of these sterilizing-grade filters is described as being hydrophilic, there was a significant difference in the hydrophobicity/hydrophilicity of the filters based on the contact angle data. The Supor EAV contact angle data was too variable for accurate analysis, with most of the measurements reporting CFE or EIPD errors. As a result, this sterile filter was not considered further in these experiments. The remaining sterile filters provided reasonable contact angle measurements and were included in the subsequent sterile filtration experiments. It is typically assumed that a contact angle greater than 90° indicates a “hydrophobic material”, while a contact angle less than 90° indicates a “hydrophilic material” [18]. Based on this crude measure, all of the filters were hydrophilic except for the Sterilux polyvinylidene fluoride

(PVDF) membrane, which was found to be slightly hydrophobic. The most hydrophilic membrane was the Supor EKV polyethersulfone membrane with a contact angle of only 37°.

Surfactant hydrophobicities were determined by the known values of the hydrophilic-lipophilic balance (HLB) for each surfactant as given in Table 2. Higher HLB values indicate more hydrophilic surfactants, while lower HLB values indicate the opposite. Given this, several combinations of surfactant and sterile filters were chosen to observe the effect of hydrophobicity on the filtration behavior of the model nanoparticle suspensions. Table 2 summarizes the filter / surfactant combinations used for these experiments.

**Table 2.** Filter and Surfactant Combinations with Rationale

| **Filter** | **Surfactant** | **Filter Contact Angle** | **Surfactant HLB** | **Rationale** |
|---|---|---|---|---|
| Supor EKV | Poloxamer 188 | 37 | 29 | Least hydrophobic combination |
| Sterilux | CTAB | 92 | 10 | Most hydrophobic combination |
| Sartobran P | Tween 20 | 45 | 16.7 | Standard reference combination |
| Stylux | Tween 20 | 51 | 16.7 | Medium hydrophobicity combination |
| Sterilux | Poloxamer 188 | 92 | 29 | Most hydrophobic filter and least hydrophobic surfactant |
| Supor EKV | CTAB | 37 | 10 | Least hydrophobic |

| | | | | |
|---|---|---|---|---|
| | | | | filter and most hydrophobic surfactant |

3.2. Comparison of 80:20 Mix to Literature Data

Initial experiments were conducted using the Sartobran P filter and Tween 20 using an 80:20 mixture of the 200 and 300 nm particles since this system has been studied extensively by Taylor et Al. [15]. As shown in Figure 5, the particle transmission initially increases with increasing volumetric throughput, which was defined as the cumulative filtrate volume divided by the membrane area. Note that a volumetric throughput of 300 $L/m^2$ corresponds to one hour of filtration based on the constant filtrate flux of 300 LMH used in this experiment. This low particle transmission at the start of the experiment was due to a combination of dilution effects associated with the buffer initially contained in the membrane and filter holder and the capture of some of the particles within specific regions of the filter. The increase in particle transmission likely reflects the saturation of many of these capture (or binding) sites. The particle transmission then passed through a maximum before decaying at higher throughput [15]. The decrease in particle transmission at high throughput is likely due to membrane fouling both within and on the external surface of the Sartobran P membrane as seen by the steady increase in transmembrane pressure throughout the filtration experiment (lower panel of Figure 5).

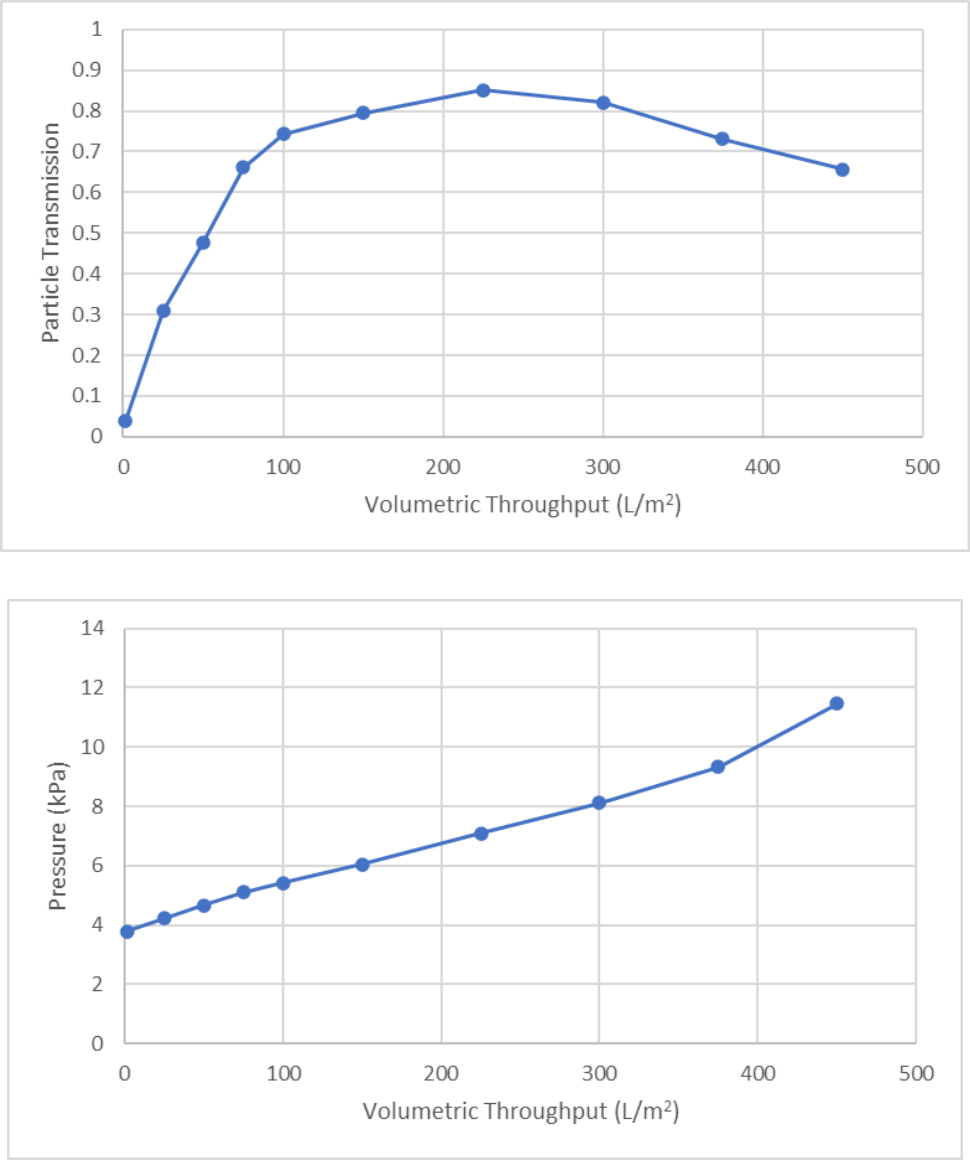


**Figure 5:** Particle transmission (top) and transmembrane pressure (bottom) as a function of volumetric throughput for the Sartobran P filter using the model nanoparticle suspension in the presence of Tween 20. Maximum throughput achieved was 450 L/m$^2$ corresponding to a filtration time of 1.5 hours at a constant flux of 300 LMH.

The behavior seen in Figure 5 closely matches that reported previously by Taylor et. al. [15] under the same experimental conditions. Taylor et al. reported a maximum in particle transmission of approximately 81% at a volumetric throughput of 250 L/m$^2$, with the particle transmission decreasing slightly at longer filtration times. Taylor et al. also reported a

nearly-linear pressure increase up to 20 kPa over 1000 L/m$^2$ of filtration [15]. The good agreement between the data in Figure 5 and that reported previously indicate that the experimental setup and methods used in this study are reliable and representative of the behavior of that observed with actual viral vaccines as discussed by Taylor et al.

### 3.3. Fouling Behavior for Different Filter and Surfactant Combinations

Membrane fouling has a host of consequences, one of which is the buildup of feed pressure [19]. Thus, a simple approach to determine fouling behavior for the different sterile filter membranes was to evaluate the transmembrane pressure profiles for each filter / surfactant combination.

Figure 6 shows data for the pressure profiles associated during filtration of the model nanoparticle suspensions at a flux of 300 LMH for the different filters / surfactants. In each case, the experiments were allowed to continue for 1.5 hours or until the pressure drop across the membrane exceeded 12 psi (83 kPa).

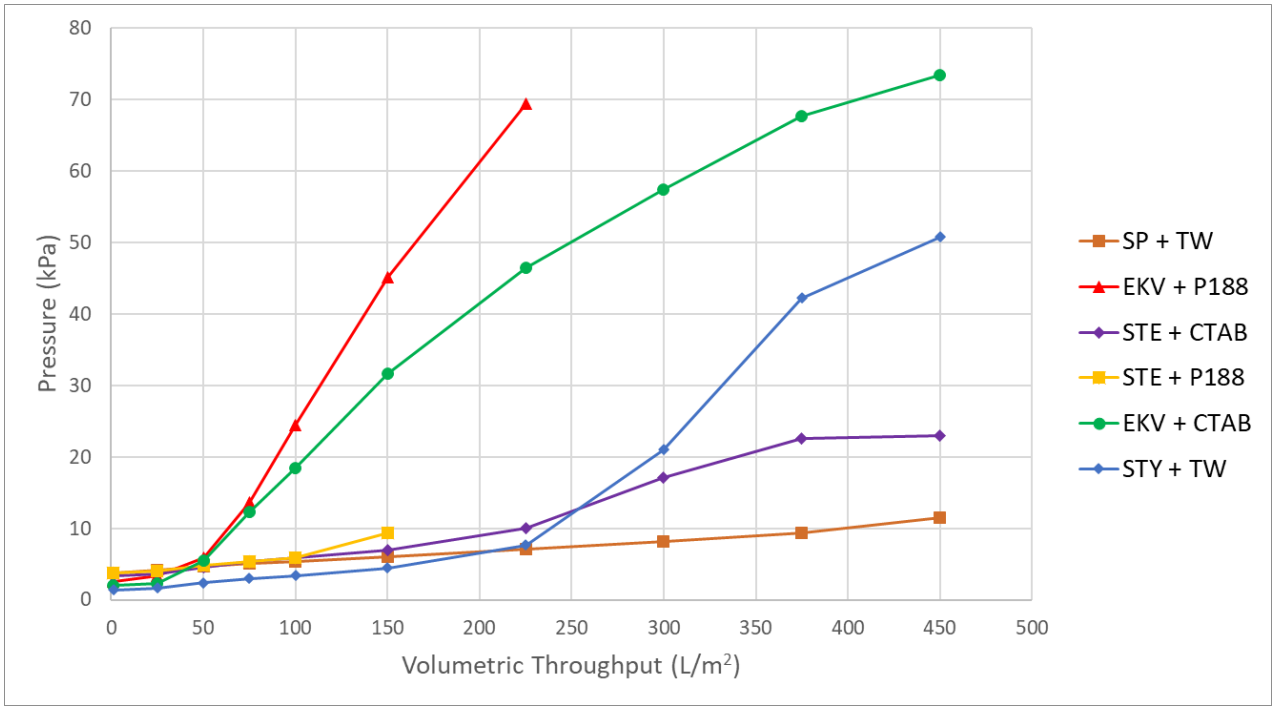


**Figure 6:** Transmembrane pressure (as a function of volumetric throughput ($L/m^2$) for the different sterile filter / surfactant combinations. SP stands for Sartobran P, TW stands for Tween 20, EKV stands for Supor EKV, P188 stands for Poloxamer 188, STE stands for Sterilux, and STY stands for Stylux. Filters are noted first, and the surfactant is noted second (after the plus sign).

The combination of the Sterilux and Poloxamer 188 exhibited notably high fouling, with experiment terminated after only 150 $L/m^2$ in throughput . This combination reflects the most hydrophobic filter with the least hydrophobic surfactant, suggesting that the filter hydrophobicity may be the dominant factor affecting the fouling behavior. Interestingly, the combination of the Sterilux membrane and CTAB surfactant displayed relatively little fouling with a maximum pressure of about 23 kPa after 450 $L/m^2$ of filtration, while the combination of the Supor EKV (the least hydrophobic filter) and Poloxamer 188 showed a high degree of fouling with a maximum of pressure of 69 kPa after 230 $L/m^2$. The significant fouling observed in both experiments using Poloxamer 188 suggests that the surfactant may be the dominant factor

controlling nanoparticle fouling in these experiments. In this case, the more hydrophilic Poloxamer 188 may have minimal binding to the hydrophobic nanoparticles, with the "bare" nanoparticles sticking to the filter material leading to a high degree of fouling. This latter behavior is consistent with results reported by Taylor et al. in the absence of any surfactant [15].

If the surfactant hydrophobicity is the dominant factor controlling fouling, it would suggest that fouling would be lowest in the presence of CTAB, the most hydrophobic surfactant examined in these experiments. However the data obtained in the presence of CTAB, denoted by the green and purple lines in Figure 6, show very different behavior. The Supor EKV membrane examined in the presence of CTAB exhibited the highest fouling of all the experiments that were run to completion, with a final pressure of 73 kPa. Meanwhile, the Sterilux membrane in the presence of CTAB exhibited the second-lowest pressure buildup of any of the experiments, with a final pressure of roughly 23 kPa. The opposite behavior in the two experiments performed with CTAB suggest that surfactant hydrophobicity alone is not the dominant factor governing the pressure buildup and membrane fouling.

CTAB is a positively-charged surfactant, thus, electrostatic interactions may also play a role in the particle filtration. In this case, the nanoparticles used in this experiment were negatively-charged and would be expected to bind easily to CTAB due to electrostatic attractions [20]. PES and PVDF are also both negatively charged membrane materials [21][22]. As a result, there is a high likelihood that electrostatic attractive interactions between the surfactant and membrane and between the surfactant and the particles contribute to the overall fouling behavior.

The results with Tween 20, which has an intermediate hydrophobicity between that of Poloxamer 188 and CTAB, also showed considerable variability depending upon the sterile filter. When Tween 20 was added to the nanoparticle suspension during filtration through the Stylux

membrane, it showed the second-highest pressure out of the experiments that ran to completion. This is in sharp contrast to the data with the Sartobran P which showed the lowest degree of fouling, consistent with results obtained by Taylor et al. This low degree of fouling was a direct result of the Tween 20. An experiment conducted using a Sartobran P filter in the absence of Tween 20 showed a much more rapid increase in the pressure (Figure 7).

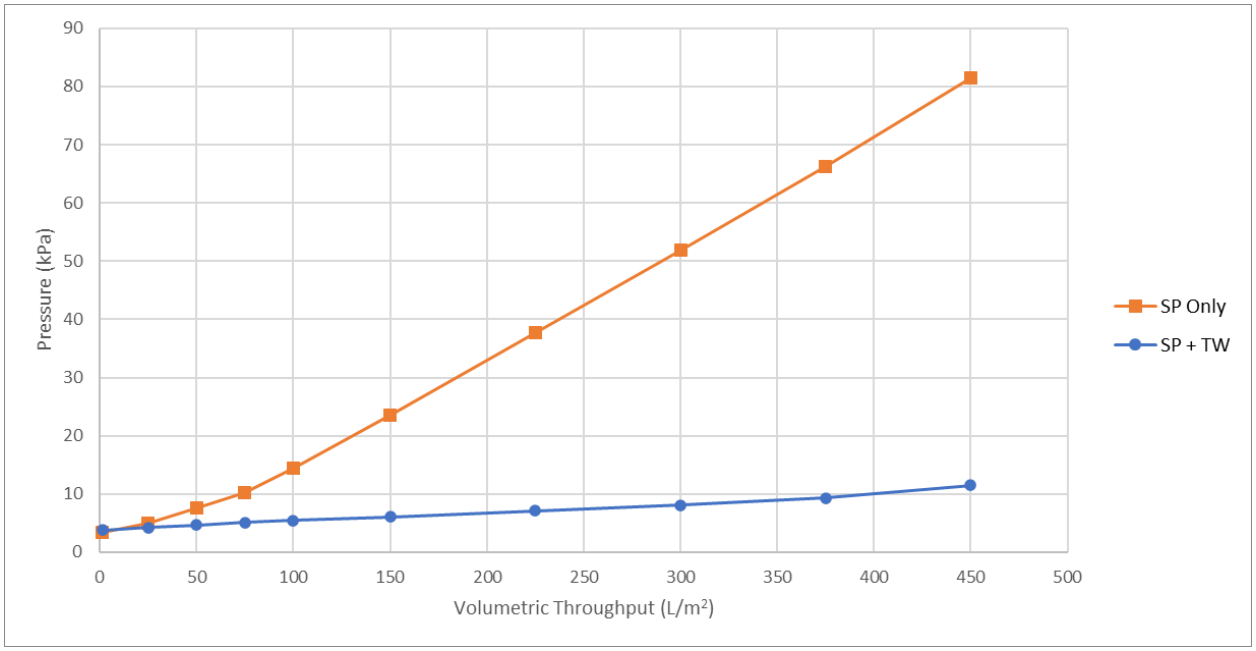


**Figure 7:** Transmembrane Pressure (kPa) as a function of volumetric throughput ($L/m^2$) during nanoparticle filtration through the Sartobran P with / without surfactant at a constant flux of 300 LMH.

The filtration through the Sartobran P reached a final pressure of 82 kPa, compared to only 11 kPa in the presence of Tween 20 due to the high retention of nanoparticles in this experiment; this will be further discussed in section 3.4. The large effect of Tween 20 on the fouling behavior of the Sartobran P was noted in past experiments as well [15]. The results of this experiment indicate a necessity for Tween 20 or some other form of surfactant, as the inclusion of a surfactant likely reduces hydrophobic interactions between the particles or

between the particles and membrane, allowing for greater transmission and lower pressure buildup [16].

In total, the experimental results in Figure 6 do not reveal any clear correlation between either the membrane hydrophobicity or the hydrophobicity of the surfactant and the observed membrane fouling behavior. The most rapid fouling occurred with the most hydrophobic filter when using the least hydrophobic surfactant, followed by the least hydrophobic surfactant and filter. The filtration experiments that showed the least -fouling were the ones using the most hydrophobic filter and most hydrophobic surfactant as well as one with a lower-medium level of hydrophobicity.

### 3.4. Nanoparticle Transmission

In addition to the increase in pressure due to fouling, the nanoparticle transmission is extremely important in a sterile filtration process. Vaccine products must be able to pass through the membrane while any bacteria that might have contaminated the product are removed. Figure 8 shows the transmission behavior of the various surfactant - membrane combinations as a function of the volumetric throughput.

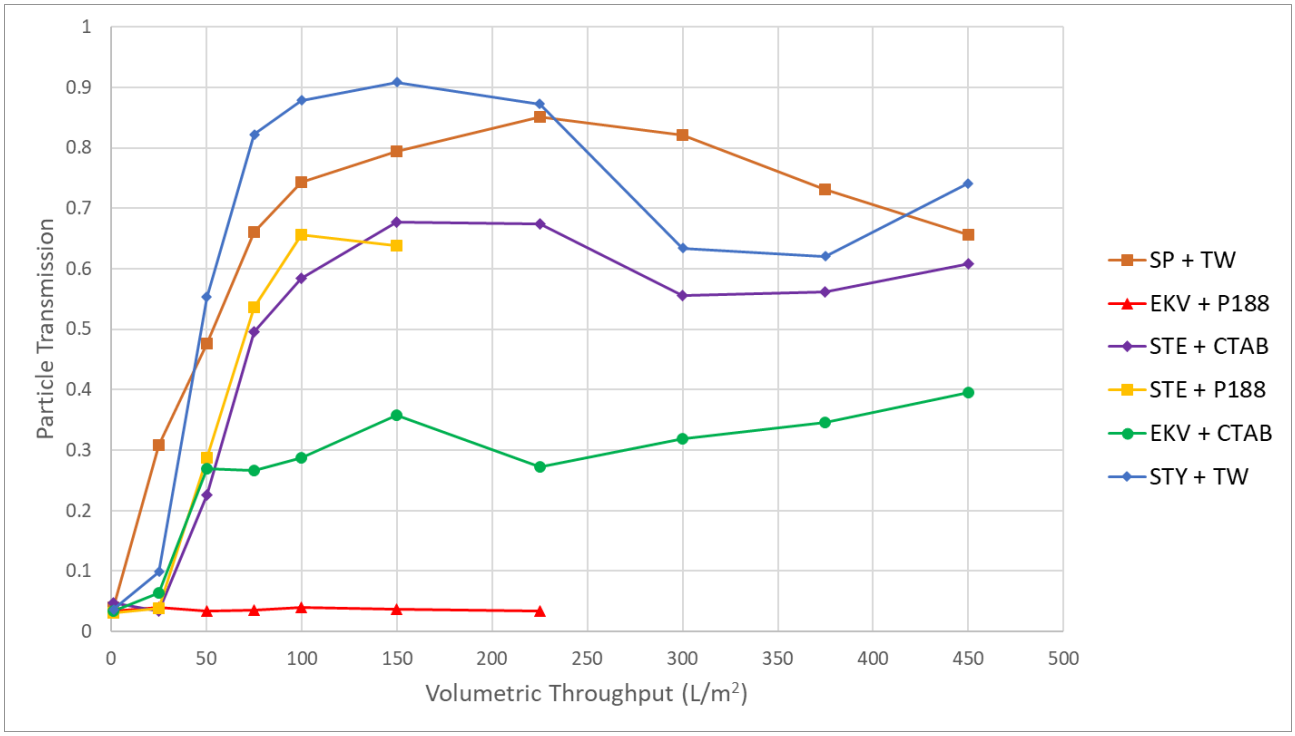


**Figure 8:** Particle transmission plotted as a function of volumetric throughput (L/m$^2$). SP stands for Sartobran P, TW stands for Tween 20, EKV stands for Supor EKV, P188 stands for Poloxamer 188, STE stands for Sterilux, and STY stands for Stylux. Filters are noted first, and the surfactant is noted second, after the plus sign.

The Stylux membrane in the presence of Tween 20 exhibited the highest particle transmission, peaking at 90% after 150 L/m$^2$ and ending at about 75% after 450 L/m$^2$. This was even higher transmission than seen with the Sartobran P / Tween 20 combination, which was the focus of the work by Taylor et al. [15].. Notably, the Sartobran P membrane in the presence of Tween 20, which represents a lower-middle hydrophobicity system, showed the next highest particle transmission. These results could suggest that Tween 20, which has intermediate hydrophobicity, is the best surfactant at increasing the nanoparticle transmission. Alternatively, the combination of membranes with intermediate hydrophobicities, when used in the presence of a surfactant having intermediate hydrophobicity, may be more effective in increasing the transmission of the model nanoparticles.

The next highest particle transmissions were obtained in the experiments utilizing the Sterilux filter, which is the most hydrophobic membrane, shown in purple and yellow. The Sterilux experiment using CTAB had a final particle transmission of 60%, with a peak transmission of about 68% at 150 L/m$^2$ in throughput. Note that the combination of the Sterilux filter and CTAB represents the membrane and surfactant with the highest hydrophobicities, again suggesting that using membranes and surfactants with relatively similar hydrophobicities encourages particle transmission. The Sterilux filtration performed in the presence of Poloxamer 188 showed similar particle transmission as that with CTAB, reaching a maximum transmission of 66%, but the rapid fouling of the membrane (rapid pressure increase) caused the experiment to be terminated after only 150 L/m$^2$ of filtration.

Finally, the Supor EKV experiments showed the lowest particle transmission irrespective of the surfactant. The Supor EKV with Poloxamer 188, which was the lowest relative hydrophobicity combination, showed only 3% particle transmission over the entire duration of the experiment out to 225 L/m$^2$. Meanwhile, the Supor EKV with CTAB never achieved particle transmission above 40%, although this filtration was able to be completed out to 450 L/m$^2$ throughput.

As mentioned previously, the particle transmission in the absence of any surfactant was quite low for all of the filters. Figure 9 shows the particle transmission data for the experiment utilizing the Sartobran P during filtration of the nanoparticle suspension without the aid of a surfactant.

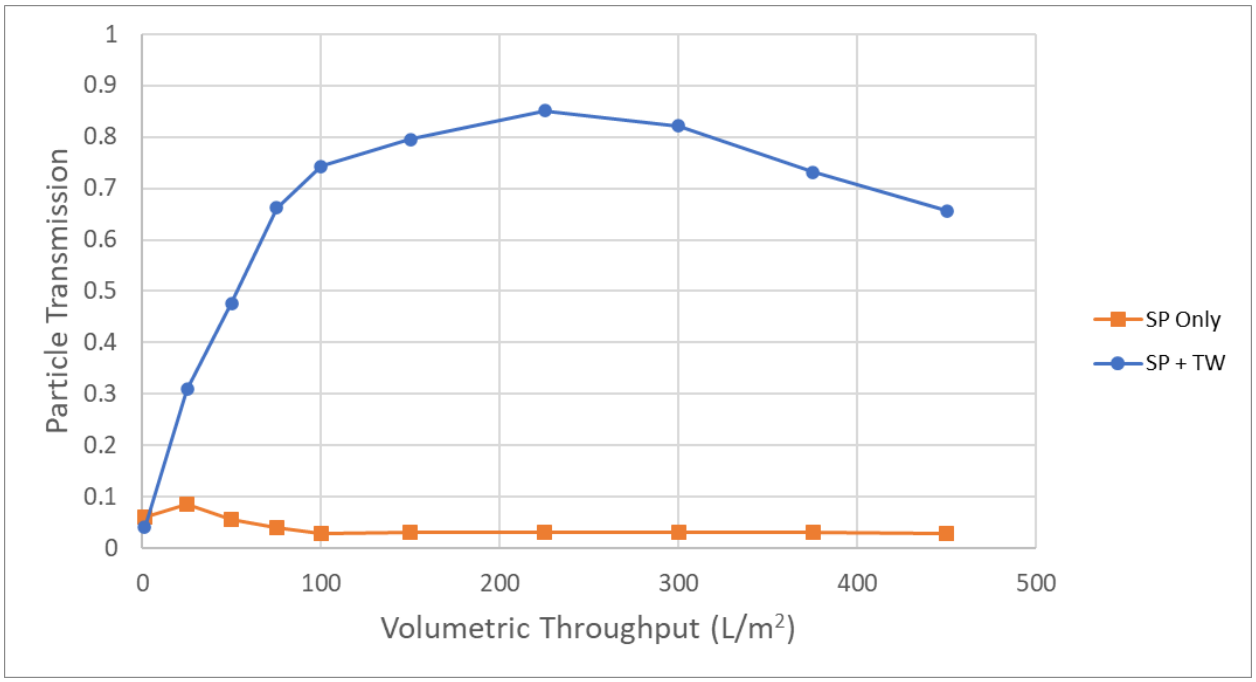


**Figure 9:** Particle transmission as a function of volumetric throughput (L/m$^2$) for the filtration of a nanoparticle suspension through the Sartobran P with / without surfactant at a flux of 300 LMH.

Even though the Sartobran P filter in the presence of Tween 20 was one of the most effective sterile filters in terms of particle transmission, this filter does not perform well in the absence of the surfactant. In this case, the maximum particle transmission was less than 10%, with the particle transmission after 25 L/m$^2$ decreasing to 3% for volumetric throughput above 100 L/m$^2$. The low transmission in the absence of surfactant versus the extremely high transmission in the presence of surfactant demonstrates the importance of the surfactant during filtration of these model nanoparticle suspensions.

The particle transmission data in Figure 8 for the different sterile filters do tend to cluster, with the lowest transmission for the Supor EKV and intermediate transmission for the Sterilux, suggesting that nanoparticle transmission may be dominated by factors outside of the membrane hydrophobicity. One such explanation for this is that the effective pore sizes of each of these

membranes may be different, despite the 0.2 / 0.22 μm standard pore size rating. A previous study has found that the average pore sizes between the filter membranes do differ, with the Sartobran P and Stylux exhibiting the largest average pore sizes of 0.445 and 0.428 μm respectively [23]. The Supor EKV possessed a smaller average pore size at 0.394 μm. These average pore sizes do match the general trend observed in Figure 8, indicating that size-exclusion mechanisms probably dominated the particle transmission behavior rather than hydrophobicity differences.

The pore size differences may also explain the weak minimum observed in the particle transmission for some filters, with the transmission rising again towards the end of the filtration experiment. This behavior was observed in all filters that were able to achieve the maximum throughput of 450 $L/m^2$ besides the Sartobran P + Tween 20. It is likely that the larger average pore size of the Sartobran P filter allowed for more of the larger 300 nm particles to pass through the membrane pores, leading to a steady increase in particle transmission until the formation of a particle cake causes a reduction in transmission at high throughput. The transmission dip in other experiments may be due to early blocking of the pores by larger particles, resulting in fewer particles passing through the membrane. The increase in transmission at very large throughput may be due to physical interactions between the particles, causing some particles to become dislodged, or to a shift in the flow distribution with more of the particles transported through larger (unblocked) pores in the sterile filter.

# 4. Conclusion

The objective of this thesis was to provide a more thorough understanding of the effects of hydrophobic interactions on the sterile filtration of nanoparticle suspensions that have previously been shown to provide a good model for the filtration of a live attenuated viral vaccine. Contact angle measurements were used to determine the relative hydrophobicities of several commercially available sterile filters. The most hydrophobic membrane was found to be the Sterilux, followed by the Durapore. Mid-level hydrophobic membranes were represented by the Stylux and Sartobran P, while the most hydrophilic membrane was the Supor EKV. These differences in hydrophobicity were, at least to some extent, a reflection of the underlying membrane polymer. The two most hydrophobic membranes (Sterilux and Durapore) are both made of polyvinylidene fluoride. However, both the Stylux and the Supor EKV, which show considerably different hydrophobicity, are both polyethersulfone.

Experimental data were initially obtained with a mixture containing an 80:20 ratio of fluorescent nanoparticles of 200 and 300 nm in size in 1xPBS with added Tween 20 during sterile filtration through a Sartobran P membrane. The results for the nanoparticle transmission and transmembrane pressure were in good agreement with data previously reported in the literature for the same system, demonstrating the validity of the experimental setup.

A series of experiments were then performed with different sterile filters in the presence of different surfactants, using combinations of filters / surfactants with very different hydrophobicity. In all cases, data were obtained for both the transmembrane pressure and the nanoparticle transmission as a function of volumetric throughput. Experiments performed in the presence of Poloxamer 188, the surfactant that was least hydrophobic, showed very rapid fouling, with the transmembrane pressure increasing so fast that the experiment needed to be

determined before reaching the target throughput of 450 $L/m^2$. The rapid fouling seen with Polxamer 188 may be due to the inability of this surfactant to effectively adsorb to the surface of the hydrophobic nanoparticles, consistent with the very poor filtration performance obtained in the absence of any surfactant. Outside of that, neither the hydrophobicity of the surfactant nor the membrane seemed to be the dominant factor governing the pressure buildup during sterile filtration of these nanoparticle suspensions.

The highest nanoparticle transmission was obtained with the Stylux and Sartobran P filters when used in the presence of Tween 20, suggesting that Tween 20 may be particularly effective in achieving high virus particle yields during sterile filtration. In addition, particle transmission seemed to be strongly influenced by the pore size of the sterile filter, with small increases in pore size causing a significant increase in particle transmission. The hydrophobicity of the surfactant and membrane had no clear effect on particle transmission for the range of experimental conditions examined in this thesis.

Future work in this area should examine a broader range of sterile filters and a larger number of surfactants in order to obtain additional insights into possible correlations may exist between the relative hydrophobicities of the surfactant and membrane and the overall filtration efficacy. Special emphasis should be placed on using surfactants that have the same electrical charge to eliminate the effects of electrostatic interactions on surfactant adsorption to both the nanoparticles and the membrane. It would also be highly desirable to study the effect of the surfactant concentration on both the transmembrane pressure and particle transmission.

Another recommendation would be to identify a more reliable / effective method for quantifying the hydrophobicity of the sterile filter membranes since the rapid intrusion of the water droplet into the membrane pores made it difficult to evaluate the contact angle. One

possible approach would be to use a pendant air bubble. In this case, the membrane is fully immersed in water, with an air bubble introduced into the system and allowed to rise until it presses against the surface of the filter. The contact angle is then evaluated between the air bubble and the membrane. The should eliminate the problems seen with the use of water droplets since the membrane pores would be fully intruded (wet with water) throughout the experiment.

# 5. References


1. Pollard, A. J.; Bijker, E. M. A Guide to Vaccinology: From Basic Principles to New Developments. *Nature Reviews Immunology* **2020**, *21* (2), 83–100.
2. Clem, A. S. Fundamentals of Vaccine Immunology. *Journal of Global Infectious Diseases* **2011**, *3* (1), 73.
3. Roberts, L. Infectious disease. An ill wind, bringing meningitis. *Science* 320, 1710–1715
4. Agarwal, R., & Gita G. (2021). A proposal to end the COVID-19 pandemic. IMF Staf Discussion Notes 2021, no. 004.
5. Vaccines market size, share, growth: Global Industry Report [2028]. https://www.fortunebusinessinsights.com/industry-reports/vaccines-market-101769 (accessed Mar 29, 2023).
6. Pfizer's financial performance in 2021. https://www.pfizer.com/sites/default/files/investors/financial_reports/annual_reports/2021/performance/ (accessed Mar 29, 2023).
7. Moderna 2021 Annual Report. https://s29.q4cdn.com/435878511/files/doc_financials/2021/q1/Moderna-1Q-2021-Earnings-PR-(05.06.21).pdf (accessed Mar 29, 2023).
8. Plotkin, S.; Robinson, J. M.; Cunningham, G.; Iqbal, R.; Larsen, S. The Complexity and Cost of Vaccine Manufacturing – An Overview. *Vaccine* **2017**, *35* (33), 4064–4071.
9. Vetter, V.; Denizer, G.; Friedland, L. R.; Krishnan, J.; Shapiro, M. Understanding Modern-Day Vaccines: What You Need to Know. Annals of Medicine 2017, 50 (2), 110–120.

10. Monreal-Escalante, E.; Ramos-Vega, A.; Angulo, C.; Bañuelos-Hernández, B. Plant-Based Vaccines: Antigen Design, Diversity, and Strategies for High Level Production. *Vaccines* **2022**, *10* (1), 100.
11. Kazilek. Bacteria overview. https://askabiologist.asu.edu/bacteria-overview#:~:text=Most%20common%20bacteria%20are%20about,are%20about%20100%20microns%20long (accessed Mar 29, 2023).
12. P. Kolhe, M. Shah, N. Rathore, Sterile Product Development, 2013
13. U.S. Dept. of Health and Human Services, Food and Drug Administration, Center for Drug Evaluation and Research: Rockville, MD, 2004.
14. Jing, Z.; Wang, S.; Xu, K.; Tang, Q.; Li, W.; Zheng, W.; Shi, H.; Su, K.; Liu, Y.; Hong, Z. A Potent Micron Neoantigen Tumor Vaccine Gp‐Neoantigen Induces Robust Antitumor Activity in Multiple Tumor Models. Advanced Science 2022, 9 (24), 2201496.
15. Taylor, N.; Ma, W.; Kristopeit, A.; Wang, S. C.; Zydney, A. L. Evaluation of a Sterile Filtration Process for Viral Vaccines Using a Model Nanoparticle Suspension. Biotechnology and Bioengineering 2020, 118 (1), 106–115.
16. Pazouki, M.; Noelle Wilton, A.; Latulippe, D. R. An Experimental Study on Sterile Filtration of Fluorescently Labeled Nanoparticles – the Importance of Surfactant Concentration. Separation and Purification Technology 2019, 218, 217–226.
17. Taylor, N. Effect of Surface Properties on Nanoparticle Filtration through the Sartobran P Sterile Filter.
18. Law, K.-Y. Definitions for Hydrophilicity, Hydrophobicity, and Superhydrophobicity: Getting the Basics Right. *The Journal of Physical Chemistry Letters* **2014**, *5* (4), 686–688.

19. Du, X.; Shi, Y.; Jegatheesan, V.; Haq, I. U. A Review on the Mechanism, Impacts and Control Methods of Membrane Fouling in MBR System. Membranes 2020, 10 (2), 24.
20. Taylor, N.; Ma, W.; Kristopeit, A.; Wang, S.-ching; Zydney, A. L. Evaluating Nanoparticle Hydrophobicity Using Analytical Membrane Hydrophobic Interaction Chromatography. Analytical Chemistry 2022, 94 (24), 8668–8673.
21. Kakihana, Y.; Cheng, L.; Fang, L.-F.; Wang, S.-Y.; Jeon, S.; Saeki, D.; Rajabzadeh, S.; Matsuyama, H. Preparation of Positively Charged PVDF Membranes with Improved Antibacterial Activity by Blending Modification: Effect of Change in Membrane Surface Material Properties. Colloids and Surfaces A: Physicochemical and Engineering Aspects 2017, 533, 133–139.
22. Hilal, N.; Johnson, D. The Use of Atomic Force Microscopy in Membrane Characterization. Comprehensive Membrane Science and Engineering 2010, 337–354.
23. Taylor, N.; Ma, W. J.; Kristopeit, A.; Wang, S.-ching; Zydney, A. L. Retention Characteristics of Sterile Filters – Effect of Pore Size and Structure. Journal of Membrane Science 2021, 635, 119436.

# Academic Vita - Alex Wee

apw5489@psu.edu
19alexwee@gmail.com

## EDUCATION

**The Pennsylvania State University- College of Engineering (Schreyer) University Park, PA**
*Bachelor of Engineering in Chemical Engineering* *May 2023 (Expected)*

## SKILLS

**Lab Techniques**

- Microplating, Solution preparation, pH balancing solutions, filtration measurements, etc.

**Languages**

- Proficient in English, Korean, and Spanish

**Computer Programs**

- Microsoft Programs, Aspen, Mathematica, ChemDraw, GIMP

## INVOLVEMENT

**Andrew Zydney Lab Group** **University Park, PA**
*Research Assistant* *January 2020 - Present*

- Research focused on the purification and sterile filtration of:
  - Fluorescent nanoparticles
  - Live Attenuated Viruses (LAV)
  - B. Diminuta
- Projects utilize aspects of both upstream and downstream process development
- Third author in paper - "Bacterial Retention During Filtration of a Live Attenuated Virus Vaccine Through the Sartobran P Sterile Filter"
  - Project involved the use of soy broth media cultures and bioreactor processes/controls

**AIChE President** **University Park, PA**
*AICHe Officer* *August 2021 - August 2022*

- Conduct weekly officer meetings
- Act as point of contact between large companies and student group
- Organize all organization events

**AIChE Academic Outreach Chair** **University Park, PA**
*AICHe Officer* *August 2020 - August 2021*

- Connect students to professors and companies via events and panels
- Provide information about research opportunities to students

**Tau Beta Pi (Engineering Society) Officer** **University Park, PA**
*Corresponding Secretary* *December 2021 - Present*

- Act as point of contact between chapter, national organization, and students
- Submit all necessary reports and forms

## HONORS & AWARDS

Elected to Tau Beta Pi, *2021-Present*
Tau Beta Pi Chapter Excellence Award *2022*
Tau Beta Pi Chapter Project Award *2022*